Simple liquids confined to molecularly thin layers. II. Shear and frictional behavior of solidified films

Eugenia Kumacheva[a] and Jacob Klein[b]
Weizmann Institute of Science, Rehovot 76100, Israel

(Received 2 September 1997; accepted 14 January 1998)

Using a surface force balance with high sensitivity in measuring shear forces we investigated the mechanical properties of thin layers of cyclohexane and octamethylcyclotetrasiloxane (OMCTS) in the gap between two smooth solid surfaces at discrete thicknesses $n=6-3$ molecular layers. At these layer thicknesses the films have undergone solidification due to their confinement (see preceding paper) and are capable of sustaining a finite yield stress upon being sheared. The sliding of the confining surfaces at mean velocity v_s across the films is characterized by a shear or frictional force F_s which varies with a characteristic stick-slip pattern. We investigate comprehensively the dependence of F_s on n, v_s, and on the applied normal forces F across the films. We find that transitions in film thickness from $n\rightarrow(n-1)$, with a consequent increase in F_s, may occur spontaneously during sliding with no change in F, corresponding to a multivalued friction force between the surfaces for a given load. The critical yield stress S for sliding at a given film thickness n increases monotonically with applied normal pressure P as $S=S_0+CP$ where S_0 is a constant of order 10^5 Pa (depending on n) and C is roughly constant and of order 1. A simple model for friction across such films which can account semiquantitatively for this behavior is introduced, based on a shear-melting mechanism using the Lindemann criterion. We find that the characteristic stick-slip behavior persists over the range of film thicknesses and the entire (large) range of mean shear velocities studied, and that over most of this range the mean shear forces are independent of v_s.
 [S0021-9606(98)51515-2]

I. INTRODUCTION

Liquids confined to molecularly thin films behave very differently to their counterparts in the bulk. Examples are ubiquitous: liquid lubricants solidify on being compressed to ultrathin layers;[1] gases trapped in nanometer-sized pores may order into crystalline arrays;[2] and simple liquids confined between solids surfaces undergo layering adjacent to each surface.[3,4] Effects that are directly related to the mechanical properties of such thin films include capillary wetting;[5] tribology, adhesion and wear phenomena,[6,7] and the microfluidity of biological membranes,[8] where water is confined by lipid bilayers. Such thin films are also implicated in the rigidity and flow behavior of granular materials,[9] ceramics,[10] and advanced composites,[11] where deformation occurs via shear of thin interfacial layers at grain or phase boundaries. At the same time, the interplay between the dynamics, thermodynamics, molecular structure of the fluids, and the commensurability and interactions of liquids in films of molecular thickness with their confining surfaces presents a continuing scientific challenge.[12,13]

Historically, an important direction in studying the mechanical properties of thin, confined solid films commenced with the microscopic investigations of friction between solid surfaces separated by lubricants. The Cambridge school in particular, starting several decades ago with the work of Bailey and Courtney-Pratt,[14] and Tabor and Bowden[6,15–17] studied frictional forces between well-defined thin solid films. More recently, several studies have investigated the shear behavior of films confined to molecularly thin films, using both surface force balance approaches,[18–23] and theoretical and computer simulation methods.[24–31] Experimentally, films of simple liquids with quasispherical molecules, as well as of liquids consisting of short linear chains, were found to behave in a solidlike manner when the films were between 1 and 3 molecular layers in thickness. This solidlike behavior manifested itself in the ability of the confined liquid to sustain a finite shear stress before yielding, and in stick-slip behavior characteristic of ductile solids. Computer simulation studies have also shed much light on the nature of the stick-slip mechanism in sheared solidlike films.[25,32]

A fundamental question concerns the manner in which thick liquid films become solidlike once they are confined to a few monolayers. In earlier work[33] and especially in the preceding paper (I),[34] we examined how a number of simple organic liquids [octamethylcyclotetrasiloxane (OMCTS), cyclohexane, and toluene] change their dynamic/mechanical properties on being confined to progressively thinner films by smooth solid surfaces. From a structural point of view, as has long been known,[3,4,35] these liquids undergo layering parallel to the confining surfaces, revealed, for example, by normal surface force measurements, as shown in Fig. 1 for OMCTS and cyclohexane. As to their dynamic behavior, we found that the liquids within the gap remain fluidlike from a macroscopic gap thickness (>1000 Å) down to surface sepa-

[a]Present address: Department of Chemistry, University of Toronto, Toronto, ON M5S 3H6, Canada.
[b]Author to whom correspondence should be addressed.

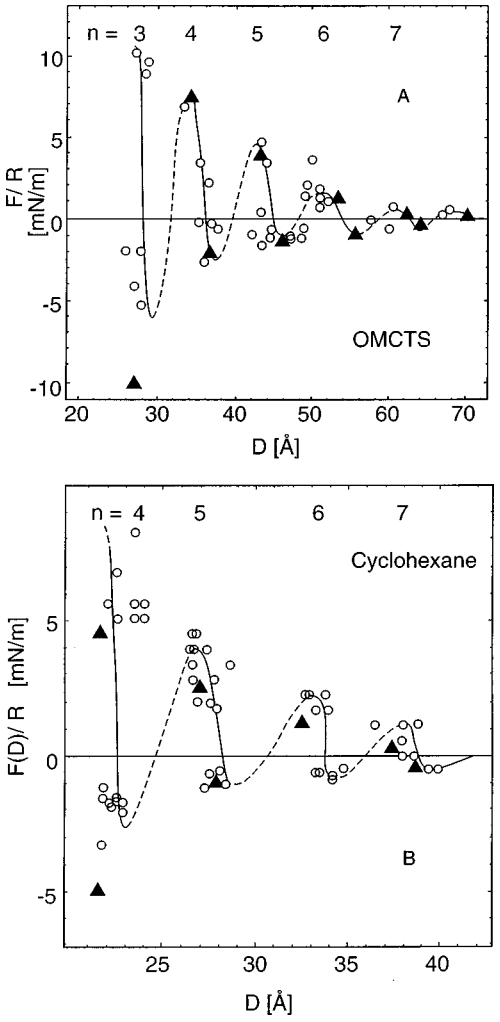

FIG. 1. (A) Force (F)-distance (D) profile between curved mica surfaces (plotted as $F(D)/R$ where R is mean radius of curvature) in a crossed cylinder configuration in OMCTS. (Solid triangles: data from Ref. 3.) (B) $F(D)/R$ profiles in cyclohexane. (Solid triangles: data from Ref. 3.) Adapted from paper I (Ref. 34).

rations D equivalent to a few, n say, monolayers of the liquid. On decreasing the gap further by a single molecular dimension, to a thickness $n=n_c$ monolayers, the confined films undergo an abrupt (first-order-like) transition to a solidlike phase. This solidity expresses itself primarily in the ability of the films to sustain a finite shear stress with no measureable relaxation over macroscopic times. Films of thickness $n \leqslant n_c$ monolayers of these liquids are all solidlike. In the present study the mechanical properties of these solidlike phases of the confined liquids are investigated in detail. We use a surface force balance (SFB) with a uniquely sensitive shear force measuring capability to probe the shear behavior of the films over a wide range of conditions. Previous investigations probed films of thickness $n=1-3$ monolayers under substantial applied compressive loads.[18–21] The much higher sensitivity of the SFB in this work enables us to examine the nature of the films, even in the absence of any applied pressure, from the point at which they just solidify as a result of confinement ($n=n_c=6$ or 7 for OMCTS and cyclohexane), and at progressively higher confinements, $n=6-3$.

In Sec. II we briefly describe the experimental approach. The main output of the experiments is the lateral stress required to shear the films, and this is investigated in Sec. III as a function of the film thickness, the external applied pressure on the films, and the rate at which the confining surfaces are made to slide past each other. We examine especially the question of critical shear stresses required to induce flow of the films, and the issue of stick-slip sliding. In Sec. IV we discuss our results, and in particular introduce a model for friction between surfaces separated by thin solid films, using a shear melting picture based on a Lindemann-type criterion.

II. EXPERIMENT

The surface force balance used has been described in detail in the preceding paper (I).[34] Basically, the liquids studied are confined between atomically smooth mica surfaces in a crossed-cylinder configuration (mean radius of curvature R). The separation D between the surfaces is measured (to ± 1 to 2 Å) using optical interference [via fringes of equal chromatic order (ECO fringes)]. The top surface is mounted on a sectored piezoelectric tube (PZT) which can provide both normal (approaching and receding) and lateral (sliding) motion of the surfaces relative to each other, by suitable variation of the potentials applied to its sectors.[34] Normal forces F or shear forces F_s across the confined films are measured by monitoring the bending of two sets of orthogonal springs on which the surfaces are mounted (one set each for each of F and F_s). At any instant the experiment measures the values of F, F_s, and the relative sliding velocity v_s, as well as the film thickness D. The data are often conveniently shown as the variation with time of the lateral motion, applied to the top surface via the PZT, together with the corresponding force transmitted across the film to the lower surface. Several examples are shown in the next section.

Cyclohexane (Fluka, analytical grade) and OMCTS (Fluka, purum grade, 99% pure) were stored for 2 days above 4 A molecular sieves and then distilled over pure, dry, filtered nitrogen. The structure and molecular characteristics of these liquids are given in Table I. In several of the experiments the liquids were twice distilled over nitrogen. For OMCTS the middle fraction boiling at 175 °C (the literature boiling temperature) was collected, and injected into the bath of the force balance (Fig. 1) under dry filtered nitrogen. The inside of the force balance was kept dry with P_2O_5. We found that for cyclohexane this distillation procedure did not result in noticeable changes relative to using cyclohexane directly from a freshly opened bottle, and in a number of the experiments this latter procedure was used. For the case of OMCTS, however, we found that careful double distillation, handling, and drying were essential for removing impurities and for observing the shear behavior of the films described in this paper.

All organic liquids used to clean the apparatus were analytical grade. Water used was purified (ELGA-Q water purification system). Sym(diphenyl carbazide) was used to glue the mica sheets to the cylindrical glass lenses for both the cyclohexane and OMCTS experiments.

Results are shown from six different experiments with

TABLE I. Structure and properties of liquids used.

Liquid	Structure and formula	Approximate diameter (Å)	Melting temp. (°C)
Octamethylcyclo tetrasiloxane (OMCTS)	$(SiO)_4(CH_3)_8$ 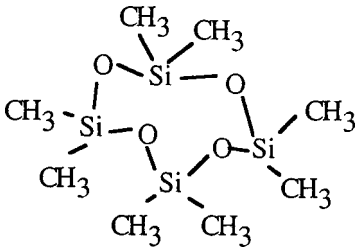	8.5–9	17
Cyclohexane	C_6H_{12} 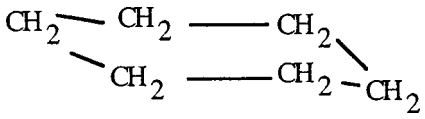	5.5	6

data often taken from several different contact points between the mica surfaces in each experiment.

III. RESULTS

A. Structural oscillations

Prior to measuring shear forces, normal force-distance profiles were measured as discussed in detail in part I. The resulting structural oscillations are reproduced in Fig. 1 (and plotted in the normalized form $F(D)/R$ versus D). Normal force profiles were also routinely measured as controls for purity throughout the experiments. Decay or suppression of the oscillatory forces were generally correlated with the presence of impurities, indicating that an experiment had to be terminated.

B. Solid–solid transitions

Following the confinement-induced liquid-to-solid transition at gap thicknesses of $n_c=6$ molecular layers, the confined phases of both OMCTS and cyclohexane displayed solidlike features also for all thinner films studied. In all cases the confined layer thicknesses were integral multiples of the molecular dimensions (Table I and Fig. 1), of thickness $n=6-3$ molecular monolayers. We found that when films of thickness $3\leqslant n\leqslant 6$ layers were sheared for a time under finite loads, they often thinned spontaneously to $(n-1)$ layers, with a corresponding marked change in their stick-slip behavior. Such behavior is shown in Fig. 2, where a film of cyclohexane of thickness 33 ± 2 Å ($n=6$) is sheared under a moderate normal stress, exhibiting clear stick-slip behavior.

Before describing such spontaneous thinning, we remark on some of the general features displayed by the lower trace in Fig. 2, which shows how the shear force across the confined films varies as the top mica surface is moved laterally (top back-and-forth trace). The maximum shear force which the film is capable of sustaining before yielding is the static frictional force opposing relative sliding of the two surfaces. As long as the shear force applied across the film (via bending of the shear springs) is lower than this value, the two surfaces slide together (the ''stick'' part of the stick-slip cycle). During the ''stick'' the shear force across the film increases as the top surface moves laterally, progressively bending the shear springs. A critical shear stress across the film is reached at the point when the shear force exceeds the static frictional force (e.g., points C or C' in the lower trace of Fig. 2). At this point the film yields and the surfaces slide (the slip part of the stick-slip cycle). During sliding stored stress is released, and at the end of the slip the film solidifies

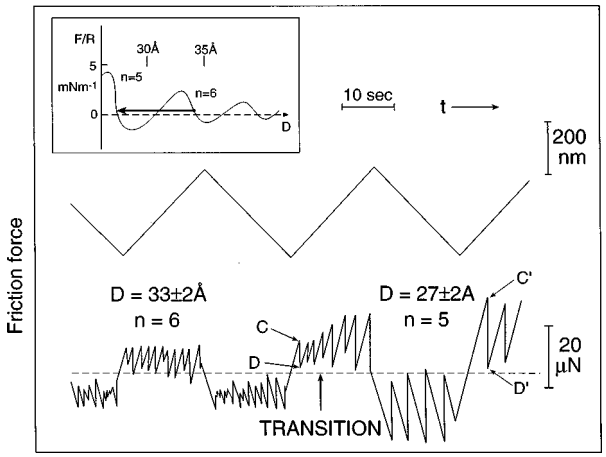

FIG. 2. Top trace is the applied motion to the top mica surface, and the lower trace is the shear force between the surfaces when separated by a film of n molecular layers of cyclohexane under a load $F/R=0.44$ mN/m. At the point shown a transition between them occurs; this is manifested in the amplitude of the stick to slip change (C-D relative to C'-D') and is noted also in the shift of the ECO fringes which shows the film thickness to change as indicated. The inset shows the transition (to scale) as a penetration across the force barrier separating the two confined phases in the cyclohexane force-distance profile [adapted from Fig. 1(B)].

again (e.g., at points D or D'), whereupon the stick-slip cycle repeats itself as long as the upper surface is still moving laterally.

In the lower trace of Fig. 2, at the point indicated, a transition in the stick-slip characteristics is observed, which becomes fully developed within some 3–5 s. At the same time a corresponding shift in the ECO fringes reveals a decrease in the film thickness from $D=33\pm2$ Å to $D=27\pm2$ Å, i.e., the effect is the result of an $n=6\rightarrow n=5$ transition. The inset to Fig. 2, drawn to scale, shows the shear-induced approach of the surfaces across the normal force barrier separating the two layers. We note especially that, while the critical shear stress for sliding increases significantly over the transition ($C\rightarrow C'$ in Fig. 2), the shear stresses at the resolidification points (D,D') remain unchanged and close to zero. The qualitative reason for the $n\rightarrow(n-1)$ transitions is presumably the facility with which the confined film, while in its liquidlike state during slipping in the stick-slip cycle, is able to squeeze out a layer of molecules under the applied pressure.

C. Shear at decreasing load: Suppression of structural forces

In general, structural forces measured with the surface force balance manifest themselves by repulsion ''maxima'' on approach of the surfaces, and jump-outs from the minima as the surfaces are made to recede. Such oscillating normal force profiles, in particular the minima in $F(D)$, as shown in Figs. 1(A) and 1(B) for OMCTS and for cyclohexane, are always measured in the absence of applied shear motion. However, when the surfaces are made to slide past each other as they recede, we find that the characteristic jump-out behavior may be suppressed. This is shown in Fig. 3 for films of initial thickness corresponding to $n=6$ and $n=5$ monolayers of cyclohexane. The surfaces are made to undergo a back-and-forth shear motion [upper traces in Figs. 3(A) and 3(B)], by applying potentials to opposing outer sectors of the sectored PZT, while at the same time the pressure between them is progressively reduced, by changing the potential of the inner surface of the PZT. We observe that, while the mean shear stresses between the surfaces decrease monotonically to zero as the pressure decreases, no accompanying ''jump-out'' is observed when F becomes negative, as is the case with unsheared films; rather, the surfaces move out smoothly to beyond the range of any detectable interaction. This suppression of the structural forces may be the result of the shear-induced ''liquification'' of the confined films during shearing, which enables smooth separation of the surfaces as they move apart. It is always observed when surfaces confining films of thickness $n=5$ or 6 are decompressed to negative loads. In contrast, in observations on OMCTS films of thickness $n=3$ ($D=27\pm2$ Å), stick-slip behavior was sometimes maintained even under an appreciable negative load (see later). This behavior may be understood in terms of the model for stick-slip motion described in the next section.

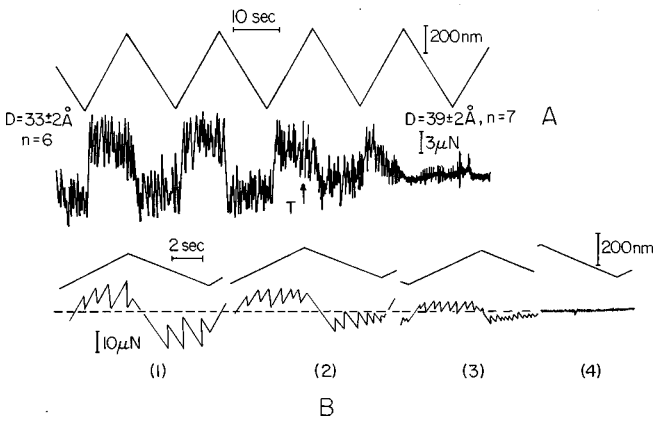

FIG. 3. (A) Top trace is the applied motion to the top mica surface, and the lower trace is the shear force between the surfaces when separated by a film of n molecular layers of cyclohexane under a decreasing load. To the left of the point T marked by the arrow $n=6$ ($D=33\pm2$ Å) and the normal load is $F/R=0.17$ mN/m. At T the load is reduced to $F/R=-0.03$ mN/m while the surfaces are still moving. The surfaces then separate to $D=39\pm2$ Å, as indicated by the ECO fringes, while the shear force decays with time as shown. No jump-out is observed as would be the case in the absence of the applied shear motion [Fig. 1(A)]. (B) The top traces are the applied motion to the top mica surface, and the lower traces show the shear force between them when separated by a film of cyclohexane. Traces 1–3 are for a film of thickness $n=5$ molecular layers ($D=27\pm2$ Å) at progressively lower loads: (1) $F/R=0.6\pm0.1$ mN/m; (2) $F/R=0.33\pm0.1$ mN/m; (3) $F/R=0.22\pm0.1$ mN/m. In trace 4 the normal load has been reduced to 0.05 ± 0.1 mN/m during the back-and-forth shear motion, and the surfaces subsequently move out smoothly to $D=60$ Å. No jump-out is observed, as noted for separation for an $n=5$ film in the absence of normal applied motion [Fig. 1(B)].

D. Critical shear stress as function of applied load

Shear stresses between the sliding surfaces across both cyclohexane and OMCTS films were comprehensively measured as a function of the film thickness and the applied normal load, from traces such as shown earlier (Figs. 2 and 3), and schematically in the inset to Fig. 4. As shown in this inset, the shear force F_s during the stick-slip motion in one direction varies between the solidification point $F_{s(\text{s.p.})}$ and the yield point $F_{s(y)}$. We may define likewise two limiting shear stress values $S_{c(\text{s.p.})}=(F_{s(\text{s.p.})}/\mathscr{A})$ and $S_{c(y)}=(F_{s(y)}/\mathscr{A})$, where $\mathscr{A}$ is the flat area of contact between

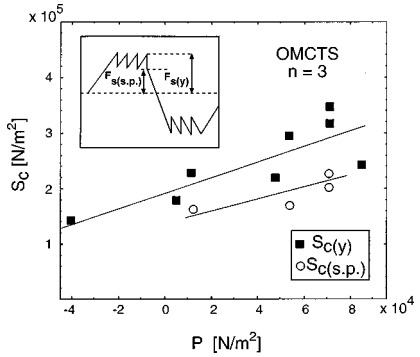

FIG. 4. Variation with pressure P of the yield shear stress $S_{c(y)}$ and the kinetic shear stress $S_{c(\text{s.p.})}$, defined as $S_{c(y)}=F_{s(y)}/\mathscr{A}$ and $S_{c(\text{s.p.})}=F_{s(\text{s.p.})}/\mathscr{A}$, where the shear forces F_s are determined from the stick-slip traces as shown in the inset, and $P=F(D)/\mathscr{A}$, where $\mathscr{A}$ is the contact area between the surfaces. Data shown for an OMCTS film of thickness $n=3$.

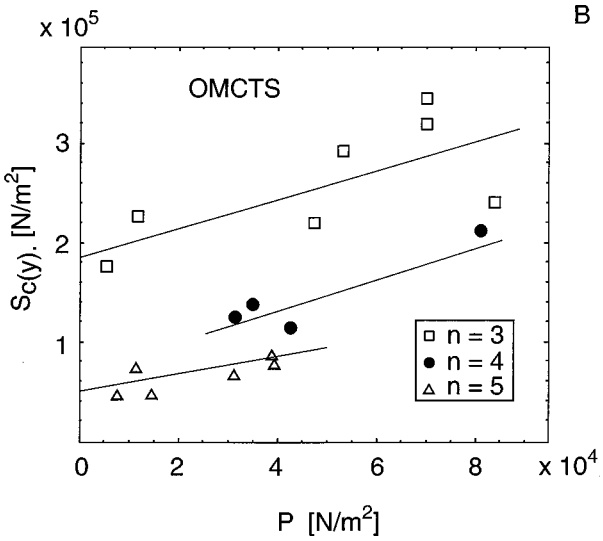

FIG. 5. Variation with pressure P of the yield shear stress $S_{c(y)}$ for OMCTS films of thickness $n=3$, 4, and 5 molecular layers as shown.

the surfaces.[36,37] Figures 4–6 and 7–9 show the variation of S_c with normal pressure $P=(F/\mathscr{A})$ for OMCTS and cyclohexane, respectively, highlighting in particular the differences between $S_{c(\mathrm{s.p.})}$ and $S_{c(y)}$, and the differences between films of different thicknesses in the range $n=3-6$. We note that P is not directly proportional to the normal load F alone, since $\mathscr{A}$ also varies with the normal load.[36] The shear stresses measured are not a sensitive function of the sliding velocity v_s (see below Figs. 10–14): the data in Figs. 4–9 were taken at relatively low velocities, in the range $v_s=20-500$ nm/s.

Figure 4 shows the variation of S_c with P for films of thickness $n=3$ monolayers of OMCTS. The film thickness (in Å) varies very slightly as a function of P (barely within the resolution of the measurements): it is in the range $D=(27 \text{ to } 28)\pm 2$ Å, and depends on the precise position on the repulsive maximum corresponding to $n=3$ on the force-

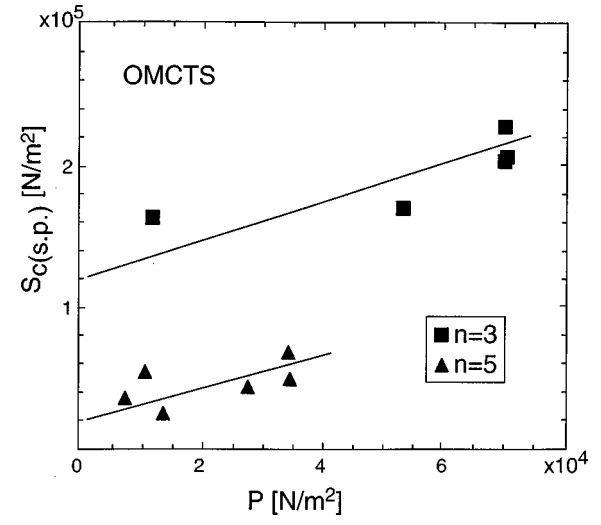

FIG. 6. Variation with pressure P of the shear stress at the solidification point $S_{c(\mathrm{s.p.})}$ for OMCTS films of thickness $n=3$ and 5 molecular layers as shown.

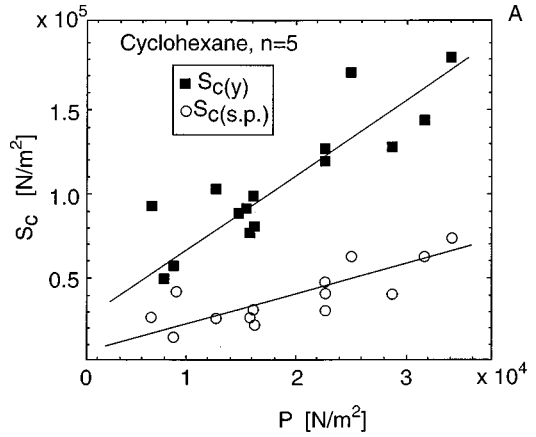

FIG. 7. Same as Fig. 4, for a cyclohexane film of thickness $n=5$ molecular layers.

distance profile for OMCTS [see Fig. 1(A)]. Similar considerations apply to the other data appearing in Figs. 4–9. In Fig. 4 we see that both $S_{c(\mathrm{s.p.})}$ and $S_{c(y)}$ increase monotonically with increasing pressure, and have finite values when extrapolated to zero normal loads. This is consistent with the adhesive nature of the contact. Indeed, for the $n=3$ film, with its particularly large adhesive minimum, Fig. 1(A), stick-slip behavior was noted even for negative applied pressures. $P<0$, as seen by the left-most point in Fig. 4. Qualitatively, the reason for this is that even for $P<0$ there is a net attraction between the surfaces (due to the large attractive well for $n=3$); this ensures that during the slip cycle the surfaces do not recede. This is related to the origin of the refreezing behavior at the end of the slip cycle, and is considered in more detail in the Discussion (end of Sec. IV B 1). An important issue related to the refreezing has to do with the time t_{slip} over which the slip takes place (the time over which the shear stress relaxes, for example, between points C and D in Fig. 2). Detailed examination of typical stick-slip cycles for different conditions suggests t_{slip} is of the order of 10^{-2} s.

Figure 5 compares the variation of $S_{c(y)}$ with P for OMCTS films with $n=3$, 4, and 5. We note that in all cases

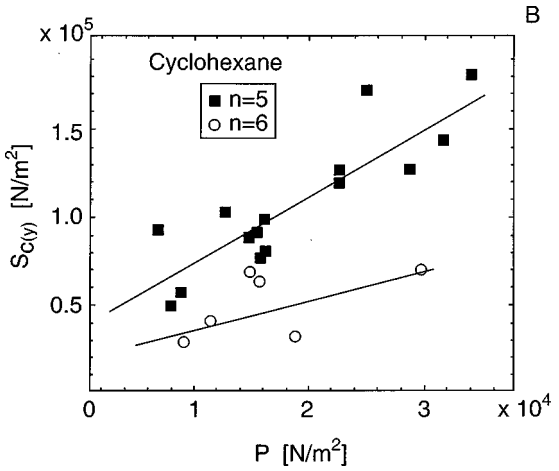

FIG. 8. Same as Fig. 5, for cyclohexane films with $n=5$ and 6.

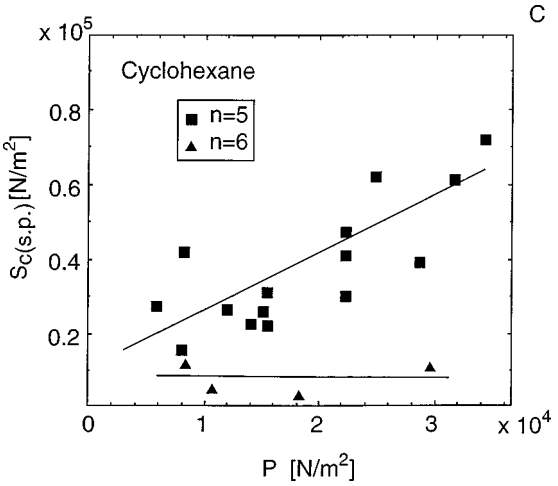

FIG. 9. Same as Fig. 6, for cyclohexane films with $n=5$ and 6.

S_c increases with P, and that at the higher n (thicker films) the yield shear stress is appreciably lower for a given P. This implies at once that for a given load, the yield shear stress is multivalued, depending on the number n of monolayers constituting the confined film. Figure 6 compares $S_{c(\mathrm{s.p.})}$ for $n=3$ and $n=5$ OMCTS films.

Figures 7–9 show the corresponding S_c vs P data for cyclohexane for $n=5$ and 6. Figure 7 contrasts the yield stresses $S_{c(y)}$ and $S_{c(\mathrm{s.p.})}$ at different pressures for $n=5$; Figs. 8 and 9, respectively, compare $S_{c(y)}(P)$ and $S_{c(\mathrm{s.p.})}(P)$ for different film thicknesses. We note that $S_{c(\mathrm{s.p.})}$ varies more weakly with pressure than $S_{c(y)}$; indeed the data for $n=6$ (Fig. 9) show little significant increase of $S_{c(\mathrm{s.p.})}$ with P (see the discussion at the end of Section IV A). The data in Figs. 4–9 show for the first time clearly the increase in the critical shear stress with applied pressure in thin films of such simple liquids. Together with the normal force profiles $F(D)$ (Fig. 1), these data specify precisely (within the experimental scatter) the yield and resolidification behavior as a function of the number of layers in each film and the normal stress within the film. In Sec. IV A we analyze the shear melting behavior and show that a simple model based on the Lindemann criterion can account well for our results.

E. Stick-slip as a function of shear velocity

The stick-slip behavior was examined as a function of the mean sliding velocity for different film thicknesses and normal loads for films of both OMCTS and cyclohexane. Figure 10 shows typical traces taken at different velocities, for a particular case (OMCTS films, $D=27\pm2$ Å, $n=3$). Figure 10(A) shows traces taken for a film under a given normal pressure ($P=7\times10^4$ N/m^2) at two different velocities, $v_s=575$ and 2000 nm/s. Clear stick-slip behavior is seen at both velocities, but the magnitude of the shear forces at the yield point ($F_{s(y)}$) are essentially unchanged. The magnitude of the forces at the point of solidification ($F_{s(\mathrm{s.p.})}$) are also similar, though somewhat smaller at the higher velocity. Figure 10(B) shows traces (taken from the recording oscilloscope) for a three-layer OMCTS film at much lower normal compression, and higher velocity ($v_s=3500$ nm/s).

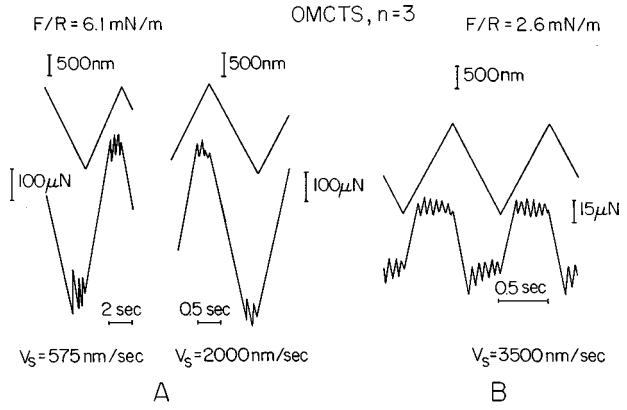

FIG. 10. Shear forces between mica surfaces across a film of thickness $n=3$ molecular layers. (A) Upper and lower traces are for the applied shear motion of the upper mica surface and the corresponding shear forces between the surfaces at two different applied shear velocities v_s as shown. Normal load $F/R=6.1$ mN/m. Traces taken from the XYt recorder. (B) Same as (A) but at a different shear velocity, and normal load $F/R=2.6$ mN/m; data recorded on the storage oscilloscope.

Here too stick-slip behavior is observed. We note especially that over the entire range of accessible sliding velocities we observed clear stick-slip oscillations during the sliding motion with well-differentiated values of $F_{s(y)}$ and $F_{s(\mathrm{s.p.})}$.

Figures 11 and 12 and 13 and 14 summarize the variation of $F_{s(y)}$ and $F_{s(\mathrm{s.p.})}$ with v_s for OMCTS and cyclohexane, respectively. In Figs. 11 and 12 we plot these for OMCTS films with $n=5$ and 3 monolayers, respectively. Within each film the normal pressure is constant (within the scatter) over the entire v_s range. For $n=5$ (Fig. 11) there is some convergence of the $F_{s(y)}$ and $F_{s(\mathrm{s.p.})}$ points as v_s increases, but they remain clearly differentiated up to the highest velocities examined. For $n=3$ (Fig. 12), at much higher normal load F, the convergence shows a similar trend but is even weaker. Figures 13 and 14 show the corresponding behavior for cyclohexane films with $n=5$, at two different normal loads. Again, there is a qualitative similarity to the OMCTS

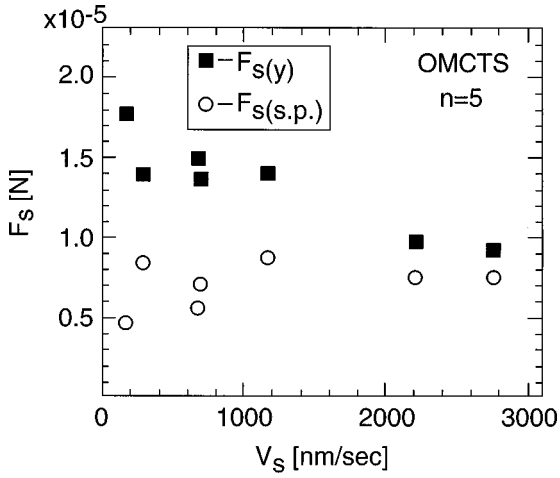

FIG. 11. Variation of yield and kinetic shear forces $F_{s(y)}$ and $F_{s(\mathrm{s.p.})}$, respectively (defined as in the inset) with applied shear velocity v_s for an OMCTS film of thickness $n=5$ molecular layers. Normal load $F/R=0.8$ mN/m.

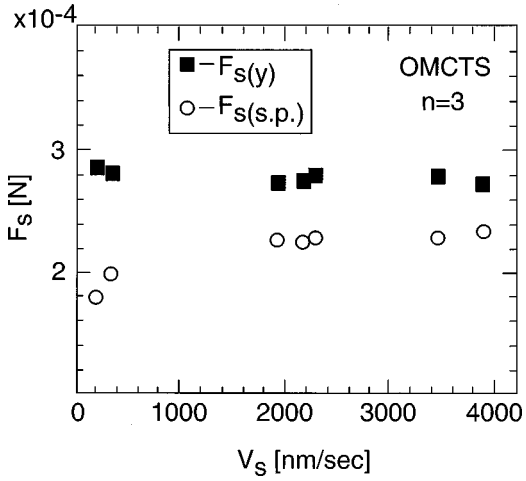

FIG. 12. Same as Fig. 11 but for an OMCTS film, thickness $n=3$ and normal load $F/R=6.14$ mN/m.

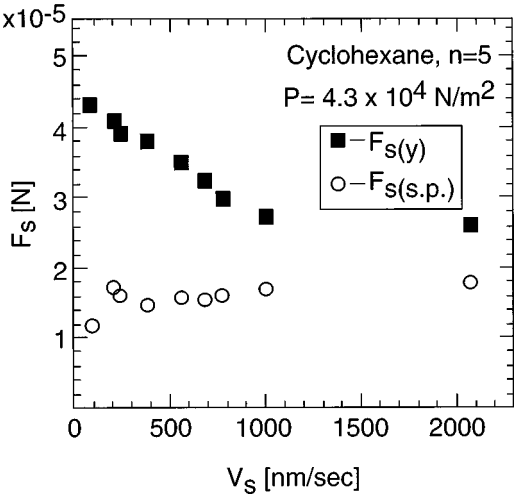

FIG. 14. Same as Fig. 11 but for a cyclohexane film of thickness $n=5$ molecular layers and at normal pressure 4.3×10^4 N/m^2.

behavior, save that the initial decrease of $F_{s(y)}$ with v_s is considerably sharper in the cyclohexane case, before leveling off at the highest velocities. The trends at both pressures are the same, though the magnitudes of the shear stresses are, as expected from Fig. 8, lower at the lower pressure (Fig. 13).

IV. DISCUSSION

The main new findings of this study derive from the increased resolution and sensitivity of the present surface force balance in measuring shear forces. This is some three orders of magnitude greater than comparable earlier studies[18–21] where monotonic shear was applied to thin confined films ($n=1-3$) at high compression. This increased sensitivity was already noted in the preceding paper I,[34] where it enabled the probing of the liquid-to-solid transition as the confinement increased from $n_c+1\rightarrow n_c$. Here the range of confined films studied was extended from the point of solidification $n=n_c$ down, that is, to thickness values $n=6-3$ monolayers. We focus on several qualitatively new features of the solidlike phase revealed at this higher resolution.

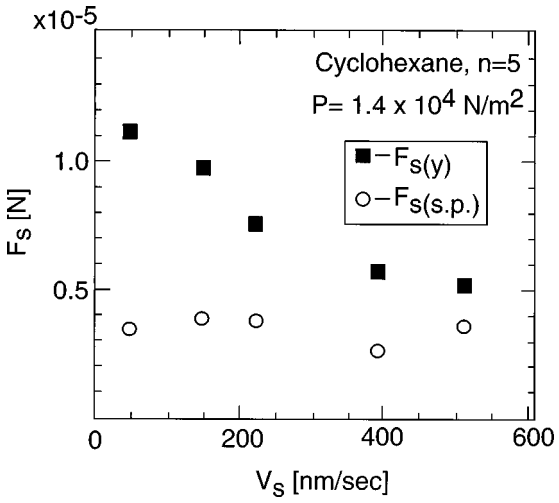

FIG. 13. Same as Fig. 11 but for a cyclohexane film of thickness $n=5$ molecular layers and at normal pressure 1.4×10^4 N/m^2.

Once the confined films have undergone solidification at $n\leqslant n_c$ they respond to shear in a characteristic stick-slip fashion, as observed earlier for a number of liquids.[20,21] However, the yield stresses for our thicker films ($n=3-6$) can be orders of magnitude weaker than have been investigated earlier for thinner, more highly compressed films.[18–20] As a first control, therefore, it is important to make contact with these earlier studies. Gee *et al.*[20] have explored the shear behavior of a number of liquids (including OMCTS and cyclohexane) compressed to film thicknesses $n=1-3$ molecular layers. This regime overlaps with ours for the case of $n=3$, and we may explicitly compare the magnitudes of the critical shear stresses obtained in the two studies for this value of n. From that study[20] we have for OMCTS, $n=3$, a critical shear stress $S_{c(y)}=1\times10^6$ N/m^2 at a normal pressure $P=(2\pm1)\times10^6$ N/m^2.[38] Extrapolating from our data in Fig. 5 for OMCTS, $n=3$, to this value of P, we find $S_{c(y)}$ in the range (1 to 2)$\times10^6$ N/m^2, the uncertainty arising from the scatter in the data. Thus for the conditions where the experimental parameters overlap, the $S_{c(y)}$ values from the earlier study by Gee *et al.*[20] [$(2\pm1)\times10^6$ N/m^2] and from this one [(1 to 2)$\times10^6$ N/m^2] agree with each other within the scatter.[39]

Several theoretical and simulation studies have also addressed the question of confined liquids under shear.[24–27,29,42,43] Although the details of the models do not always closely match the experimental conditions, these studies have cast revealing light on the process by which breakdown of the films may occur on shear. An important aspect of the films which cannot be revealed directly by the shear experiments concerns the molecular structure, both while the film is capable of sustaining a shear stress and also when it has broken down (during the slip part of the cycle). While the molecules are known to be layered parallel to the confining surfaces, little is known experimentally about their in-plane ordering. As pointed out clearly in our preceding

paper (I),[34] layering in itself does not necessarily imply that the films are solidlike. A useful measure of in-plane ordering is the Debye–Waller factor (DWF), defined in terms of the two-dimensional structure factor within a layer, whose value is unity in a perfect crystal at zero temperature, and drops to 0.6 at the melting point. Molecular dynamics simulations by Thompson *et al.* of the shear of simple liquids have indeed indicated stick-slip behavior,[25] in agreement with experiments.[1,20,22] These simulations indicate solidlike structure (DWF$>$0.6) while in the ''stick'' phase, with liquidlike structure (DWF$<$0.6) in the ''slip'' phase, i.e., a shear-induced melting of the confined films. One additional feature suggested by these simulation studies,[25] which we return to later, concerns the dilatancy effect, long known for shear of granular materials:[44] During the liquidlike slip part of the stick-slip cycle (e.g., $C \rightarrow D$ in Fig. 2) the surfaces move slightly apart, only to return to their original separation when they refreeze at the solidification point.

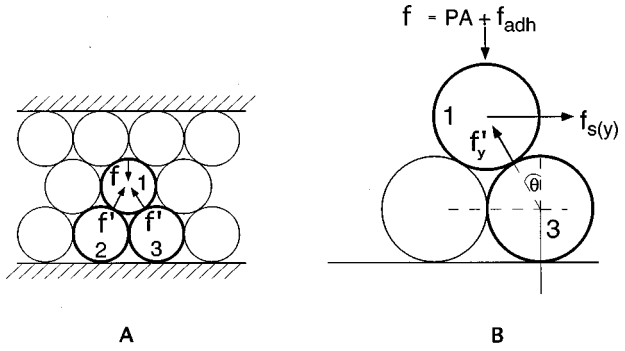

FIG. 15. Illustrating schematically the shear-melting model for friction described in the text. (A) In the absence of a shear force the normal forces f on any molecule 1 are balanced by the reaction on it due to forces f' exerted on it by each of the two molecules 2 and 3 below it (in a 2-D representation). (B) At the critical yield point under a shear force $f_{s(y)}$ (per molecule) the entire reaction on 1 is due to the reaction force f'_y due to 3, and molecule 1 is about to start sliding up molecule 3.

A. Variation of shear stress with pressure and with film thickness (Sec. III C and III D)

Figure 4–9 show the variation of the shear stress S_c for sliding as a function of the applied normal pressure P for both OMCTS (Figs. 4–6) and cyclohexane (Figs. 7–9). The yield stress, $S_{c(y)}$, corresponding to the point at which the film reaches the top of the ''stick'' cycle, increases with normal pressure over the range studied for all layer thicknesses. Within the scatter, the data may be described by a linear relation of the form

$$S_{c(y)} = S_{co} + CP. \tag{1}$$

Here $S_{co}(n)$ is the (extrapolated) value of the critical shear stress at zero applied pressure, which depends on the thickness n of the confined film, and C is a constant. A form similar to this was first proposed[17,45–47] to describe boundary friction of two solid hydrocarbon surfaces (fatty acid monolayers) sliding past each other, where for high loads (such that $CP \gg S_{co}$) C is the effective friction coefficient. It is of interest to contrast the case of boundary lubrication with that of shear of simple liquids solidified by confinement to thin films, as in the present study.

For OMCTS, for which there is more extensive data (Fig. 5), we see that while $S_{co}(n)$ varies systematically with the thickness n (molecular layers) of the confined film, the slope C is approximately constant (for $n=3,4,5$), with a value in the range $C \approx 1 \pm 0.4$. This is much larger than the value $C \approx 0.03$ to 0.04 for the boundary friction between surfaces coated with classic boundary lubricants such as fatty acid monolayers.[17] The value of the critical shear stress at zero applied pressure is also different for the two cases: $S_{co} \approx 10^6$ N/m^2 for the fatty acid monolayers, but $S_{co} \approx 10^5$ N/m^2 for the OMCTS films (depending on the number of confined monolayers n). The differences must originate in the molecular mechanisms involved in the sliding process. In the case of the boundary lubricants, sliding between them occurs exclusively at the interface between the two layers, when the interfacial contacts (due to van der Waals forces) are sheared:[46] the shear strength of this interface varies only weakly with pressure, resulting in a small effective friction coefficient C. At the same time, van der Waals attraction between the boundary lubricant monolayers leads to the adhesive interaction at zero applied load, and is responsible for the value of S_{co}.

A relation similar to Eq. (1) also describes the frictional force between a moving surface sliding above a stationary one across a film of n monolayers of linear alkanes[20] and a simple model[48] extending the classical Coulomb approach (designated the cobblestone model) has been used to describe this friction.

For the confined (solidified) simple liquids described in this study our data, as well as theoretical studies[25,26] indicating melting of the liquid at the yield point, suggest that insight into their shear behavior requires a different approach. Initiation of sliding, we believe, is associated with melting of the confined solidlike film across the entire gap, and the critical stress required to inititiate sliding is then the shear stress required for such melting. We may attempt a simple model of this as follows. We assume our film is of thickness n hard-sphere molecules solidified by confinement to a close-packed structure and that a Lindemann-like criterion applies for its melting. This postulates that when the molecules of a crystal fluctuate from their mean position by a certain fraction of the equilibrium lattice spacing, then breakdown of the entire lattice follows and melting occurs. Usually this is understood to be due to the effect of increasing temperature, but here we assume it is induced by shear.[49] The model is illustrated in Fig. 15, and we will use it to evaluate the critical, or yield shear force $F_{s(y)}$ between two surfaces just as the top one is about to start sliding relative to the bottom one.[50] This yield shear force corresponds to $F_{s(y)}$ at the top of the stick regime as defined in the inset to Fig. 4.

Consider first the situation in the absence of any shear force, Fig. 15(A). The normal force f on a given molecule (1 say) is given by the sum of the applied load PA and the net adhesive force per molecule $f_{\mathrm{adh}}(n)$. P is the pressure applied to the top surface, and A is the cross-sectional area of the spherical molecule ($=\pi\sigma^2$ where σ is its radius), while

TABLE II. Critical shear stresses and their pressure variation, comparison of experiment with the shear-melting model.

Liquid	n	C[a]	tan θ[b]	S_{co}[a] (10^5 N/m^2)	[c]$(F_p/\mathscr{A})\tan\theta$ (10^5 N/m^2)
OMCTS	3	1.4±0.4	~0.7	1.8±0.4	0.8±0.3
	4	1.4±0.4	~0.7	0.7±0.2	0.6±0.2
	5	0.8±0.2	~0.7	0.5±0.15	0.5±0.15
Cyclohexane	5	3 ±1	tan θ_{CH}	0.5±0.2	(0.6±0.2)tan θ_{CH}
	6	1.5±0.5	tan θ_{CH}	0.2±0.07	(0.5±0.2)tan θ_{CH}

[a]Based on fit of Eq. (6), $S_{c(y)}=S_{co}+CP$, to data of Figs. 4–9.
[b]Based on Eq. (5). Taking a ''2-D'' close-packing model, $\theta=30°$ (see Fig. 15). More realistic close-packing of spheres gives $\theta\approx36°$. The value of tan θ for OMCTS is based on the latter. For cyclohexane $\theta=\theta_{CH}$ may differ (see text).
[c]$F_p(n)$ is evaluated from Figs. 1(A) and 1(B), while $\mathscr{A}$ is evaluated from the JKR model (Ref. 36).

$f_{\rm adh}(n)$ is due to the attractive well associated with the structural forces for an n-layer film (Fig. 1). i.e.,

$$f=f_{\rm adh}(n)+PA. \tag{2}$$

In the absence of shear, this normal force is balanced by the reaction due to the lower molecules (2 and 3) on which the molecule rests [Fig. 15(A)], so that

$$f=2f'\cos\theta$$

(for convenience we deal with a 2-D situation as in Fig. 15: in a close-packed model a given molecule rests on 3 rather than 2 other molecules, and so on, but this makes little difference to the treatment). We now apply a progressively increasing shear stress S to the top surface. The film can initially sustain such a stress without shearing (in our model the molecular layer in contact with each surface is pinned laterally at the surface, and cannot slide smoothly past it), and so S is transmitted across each molecular layer to the lower surface: This is the ''stick'' region of the stick-slip cycle. The horizontal (shear) force on our molecule of interest 1 is then given by $f_s=SA$. As f_s increases, the reaction between 1 and 2 decreases, while that between 1 and 3 increases until the point just before molecule 1 is about to slide up molecule 3, Fig. 15(B). At this point $f_s=f_{s(y)}$, the yield shear force per molecule, the reaction force between 1 and 3 is f_y, while the reaction between 1 and 2 is zero. If we assume the spherical molecules may slide tangentially smoothly past each other, the entire horizontal force $f_{s(y)}$ acting on 1 is then balanced by the reaction due to 3. That is,

$$f_{s(y)}=f'_y\sin\theta. \tag{3}$$

The vertical component of the force between molecules 1 and 3 must balance f, that is, $f=f_y\cos\theta$. Substituting from Eqs. (2) and (3) gives

$$f_{s(y)}=(PA+f_{\rm adh}(n))\tan\theta. \tag{4}$$

The left-hand side (LHS) of (4) is the applied lateral force per molecule at the point where sliding motion is about to start, while the right-hand side (RHS) is the balancing reaction. As soon as molecule 1 starts to slide up molecule 3, θ decreases and the forces are no longer in balance: once sliding is initiated the force resisting it decreases, and distortion of the lattice occurs rapidly until melting occurs by the Lindemann criterion. The confined film is then liquidlike: it can no longer sustain the shear stress and the surfaces slide (the slip part of the cycle); the shear stress relaxes [to the value equivalent to $S_{c(\rm sp)}$ in our experiments] and the film solidifies again. We may therefore take the critical value of the shear force in Eq. (4), the point at which the molecules start to slide, as that at which the solid will distort catastrophically and melt. The critical yield stress is then given by $S_{c(y)}=f_{s(y)}/A$, i.e.,

$$S_{c(y)}=(f_{\rm adh}(n)/A)\tan\theta+P\tan\theta. \tag{5}$$

This has the form of the experimental relationship of Eq. (1) above, with tan θ corresponding to the ''friction coefficient'' C. For the close-packed configuration of Fig. 15 (in 2-D) $\theta=30°$, so that tan $\theta\approx0.6$. (For a 3-D close-packed configuration, θ is higher; see below and caption to Table II). The term $(f_{\rm adh}(n)/A)\tan\theta$ corresponds to $S_{co}(n)$ in Eq. (1), the value of the critical shear stress at zero applied pressure. $f_{\rm adh}(n)$ is directly related to the depth of the attractive well of the nth structural oscillation of the normal forces (see Fig. 1), as

$$\begin{aligned} f_{\rm adh}(n)/A&=(\text{adhesive attraction/molecule})/\\ &\quad(\text{area per molecule})\\ &=(\text{adhesive force between surfaces})/\\ &\quad(\text{contact area between surfaces})\\ &=F_p/\mathscr{A} \end{aligned} \tag{6}$$

so that $(f_{\rm adh}(n)/A)\tan\theta$ may be estimated from the pulloff force F_p corresponding to the attractive well at the relevant value of n (Fig. 1). The area $\mathscr{A}=\pi a^2$ is evaluated from the JKR model[36] at zero applied pressure.

In Table II we compare the experimental values of S_{c0} and C with the predictions of this model for several values of n, for both OMCTS and cyclohexane. We first examine the case of OMCTS, where the assumption of spherical molecules is likely to be better than for cyclohexane. Our prediction tan $\theta=0.73$ for the ''friction coefficient'' (if a spherical-close-packed (SCP) structure is assumed for the solidified molecules) is in rough agreement with the range of experimental slopes C for OMCTS (2nd column of Table II).

The predicted values of S_{co} show the right trends and are also quantitatively close to the measured values (compare the last 2 columns in Table II). The agreement with the data for cyclohexane is more qualitative: the predicted magnitudes of C and S_{co} are of the right order, and the latter reproduce the observed trend of the data. Cyclohexane has a more oblate structure than OMCTS, and the angle $\theta=\theta_{CH}$ (Fig. 15) connecting the midpoints of the molecules could be larger than for an SCP structure. In our model this would result in a larger value (tan θ) predicted for the constant C (relative to an SCP structure), as indeed observed, but in view of the simplicity of the model and the complexity of the actual detailed shape and packing of the molecules it would not be appropriate to pursue this further.

An important aspect of this model relates to the question of frictional energy dissipation as the top surface is made to slide (at a mean sliding velocity v_s) across the lower surface (against a mean friction force F_s). During the stick part of a stick-slip cycle, external work is done on the system (stretching of the shear spring on which the upper surface is mounted), but there is no frictional dissipation since there is no relative motion between the surfaces. Once the confined film liquifies at $S=S_{c(y)}$ the surfaces undergo mutual sliding as the top surface accelerates. Some dissipation then occurs due to viscous shearing of the liquid, while at the same time the top surface and its mount accelerates and gains kinetic energy. One may show[51] that in the conditions of our study the viscous dissipation is small compared with the kinetic energy imparted to the moving top surface during the slip. At the end of the slip motion the film refreezes, and the upper surface stops abruptly (the shear force at that point has relaxed to the value $F_{s(\mathrm{sp})}$). The kinetic energy associated with the rapid ''slip'' motion of the upper surface relative to the lower one is then, at the instant of resolidification and stopping, converted into other forms of energy. Solving the associated equations of motion shows explicitly[51] that the rate v_sF_s of frictional work done in sliding the upper surface can be accounted for if this kinetic energy is dissipated, as decribed above, as heat in the form of phonons generated in the upper and lower surfaces. It is of interest that, as shown in Figs. 13–15, the stick-slip behavior persists over the entire range of velocities studied, suggesting that this dissipation mechanism indeed holds throughout the conditions of our study.

The last point concerns the magnitude of the shear force $F_{s(\mathrm{sp})}$ at the solidification point (inset to Fig. 4). This is the point at which the slip regime ends and the confined film, having been liquified by shear at the yield point, becomes solidlike again. We suggest the following mechanism. It has long been known that shear of an ordered array of particles can lead to a dilatational effect,[44] and we believe this occurs also when the confined film undergoes shear-induced melting [when the shear force reaches the yield point $F_{s(y)}$]. Computer simulations show precisely such a dilatation for thin films sheared between two plates.[25] The dilatation may also be viewed as resulting from the density difference between the solid and the liquid (typically around 5% or less for a range of materials). This dilatation or density reduction in the film must manifest itself in the increased separation of the surfaces, from D to $D+\delta D$ say, just as the film melts. A 5% dilatation would correspond to δD of order 1 Å or less for D around 5 nm. Such a change in D would be difficult to observe from the motion of the ECO fringes.

Immediately following the melt transition the two surfaces begin to slide relative to each other driven by the shear force F_s, and at the same time to approach each other under the normal force F. After a time t_{slip} the surfaces have approached (by δD) D again, the density becomes once again commensurate with a solidlike behavior under confinement, and the film resolidifies. By solving explicitly the equations of motion of the two surfaces in the sliding and in the approach direction it is readily shown[51] that over the time t_{slip} the surfaces can *slide* relative to each other by an amount Δx of some nm to some tens of nm, while they *approach* only by an angstrom or so. (The reason for this is the large hydrodynamic resistance to approach of the surfaces when they are very close together, relative to the much weaker viscous forces opposing sliding). This is precisely in line with our observations. The extent of sliding Δx prior to solidification then determines the relation between the yield and the kinetic shear forces: $F_{s(\mathrm{sp})}=F_{s(y)}-K_1\Delta x$, where K_1 is the shear spring constant. According to this picture the resolidification is determined by the point where the dilatation of the confined liquid has been eliminated, rather than by the point where the shear stress has dropped to some particular value. This at once explains the apparently paradoxical ''overshoot'' of $F_{s(\mathrm{sp})}$ to negative values occasionally observed (e.g., LHS of lower trace in Fig. 2) during a stick-slip cycle. The dependence of $F_{s(\mathrm{sp})}$ on the normal force (shown in Figs. 11 and 12) can be discussed in terms of this picture, as is done in more detail elsewhere.[51] We remark finally that a detailed analysis[51] of the sliding of the surfaces during the stick-slip cycle indicates that the effective viscosity of the shear-melted liquids during the slip regime is at most of order $30P$ (for OMCTS, $n=3$).

B. Multivalued friction and solid-solid transitions (Sec. III B)

An interesting corollary of the above model is the possibility of multivalued friction over certain ranges of the normal load due to different values of $S_{co}(n)$. As long as the applied normal load is below the value corresponding to the ''hump'' of the nth structural oscillation (see Fig. 1), there are $(n+1)$ equilibrium surface separations, where the normal force is balanced by intersurface repulsion, at the $(n+1)$ discrete film thicknesses corresponding to films of thickness $0\rightarrow n$ molecular layers. As the pressure increases, jumps occur from the peak of the nth oscillation to the $(n-1)$th oscillation (it is also possible, as indicated in Fig. 2 for the $n=6\rightarrow n=5$ transition, and discussed below, for a process to occur whereby the equilibrium surface separation (n) changes even at constant pressure below the peak of the structural force oscillation). As seen clearly from data shown for OMCTS in Fig. 5 (and for cyclohexane in Fig. 8), there are different discrete values of the yield stress $S_{c(y)}$ required to slide the surfaces, corresponding to the different n values of the confined film thicknesses. These correspond to different effective friction coefficients (defined as the ratio of

shear-force required for sliding to the applied load). As the normal pressure P increases, and progressively exceeds the repulsive humps of films with higher n values, the number of possible values of the effective friction coefficient decreases (from 3 to 2 to 1, in Fig. 5), as expected.

Passage between two values of the friction is brought about by a solid-solid transition, as shown in Fig. 2 for confined cyclohexane. In contrast to the liquid-to-solid transition induced by progressive confinement alone (discussed in I[34]), such solid-solid transitions are associated with shear of the confined films: the surfaces slide back and forth with respect to each other under a given (low) load (see inset to Fig. 2), showing a characteristic stick-slip behavior with a certain magnitude of the critical yield stress. At the point marked, an abrupt transition occurs in the properties of the confined solid: The yield shear stress increases, and at the same time the spacing between the surfaces, as revealed by the ECO fringes, decreases from that corresponding to $n=6$ layers of cyclohexane (33 ± 2 Å) to $n=5$ (27 ± 2 Å), as a layer of molecules is expelled. No additional normal pressure is associated with the transition, which may be viewed as penetration between the two adjacent humps as shown in the inset to Fig. 2. Such transitions during sliding between $n=2$ and $n=1$ (for confined OMCTS films) have been noted in earlier studies,[18,52] though often only when the applied pressure was increased during the course of the sliding motion.[53]

The time scales associated with the $n=6\rightarrow n=5$ transition shown in Fig. 2 are of order 1 to 2 s or so for the stick-slip pattern (for $n=5$) to be fully developed. This contrasts with the earlier observation[20] of some 3 min required for full development of the $n=2\rightarrow n=1$ transition for OMCTS under strong compression, or some 30 s for the $n=3\rightarrow n=2$ transition in cyclohexane.[18] The difference in time scales is probably due to the sluggish dynamics associated with the more confined liquids. A longer ''massaging'' of the highly compressed $n=1$ OMCTS film appears to be required to attain the configuration associated with fully developed stick-slip motion[20,21] than is the case for the $n=5$ cyclohexane film under low compressive load. The rapid relaxation at the higher n values is consistent also with the very short time (<0.5 s) required for the liquid-solid transition (when $n=7\rightarrow n=6$) discussed in I.[34]

C. Variation of shear stress with shear rate (Sec. III E)

In paper I it was shown that the mean yield stress across OMCTS films just following the liquid-to-solid transition, $n=6$, was essentially independent of the sliding velocity v_s over a 40-fold variation in v_s. The weak dependence of the shear stress S_c on the shear velocity is seen also for thinner films. It is particularly marked in Fig. 12 (black squares), for OMCTS films with $n=3$ ($D=26\pm2$ Å) which shows the variation of the force F_s required to slide the surfaces with shear velocity v_s. The mean shear force, and hence the shear stress S_c, is nearly independent of the shear velocity over the entire range of v_s (corresponding to shear rates $\dot{\gamma}$ in the range $75-1500\ \mathrm{s}^{-1}$), i.e., $S_c\propto\dot{\gamma}^0$. Such behavior is characteristic of the shear of a ductile solid[54] rather than of a liquid. If nonetheless a Newtonian relation $S_c=\eta_{\mathrm{eff}}\dot{\gamma}$ were assumed for an ''effective viscosity'' η_{eff} of the sheared films, one could extract the variation of this ''effective viscosity'' with the shear rate (with the caveat that for films that are solidlike the Newtonian definition we use for η_{eff} is not really appropriate). Clearly, since the shear stress is independent of the shear rate, $\eta_{\mathrm{eff}}\propto\dot{\gamma}^{-1}$ over this range for the confined films,[58] for both OMCTS and for cyclohexane (see, e.g., Figs. 13 and 14).

D. Variation of stick-slip behavior with sliding velocity (Sec. III E)

The final issue for discussion concerns the variation of stick-slip behavior with shear velocity in the solidlike regime. Stick-slip classically arises when static friction is greater than kinetic friction.[1] In recent years years it has been extensively discussed[20–22,24,25,29,30,32,42] in the context of the shear of ultrathin confined films of simple liquids (such as OMCTS), where it has been viewed as related to a melting/freezing transition, and of more complex molecules (e.g., linear or branched alkanes). The possible existence of a critical shear velocity v_c at which the stick-slip behavior disappears is intriguing, and has been described in a number of studies.[20,21] A simple expression for the critical velocity was proposed by Robbins and Thompson,[55] arising from their computer simulations of the sliding of a plate of mass M across a thin film of simple liquid of molecules of size σ. Their expression for the critical velocity was

$$v_c=\mathrm{const}\sqrt{\frac{F_{s(y)}\cdot\sigma}{M}}, \tag{7}$$

where the value of the constant is in the range 0.05–0.5.[56]

Figures 10–15 show the effect of varying the shear velocity both on the yield shear force $F_{s(y)}$ and on the kinetic shear force $F_{s(\mathrm{sp})}$, for both OMCTS and cyclohexane at different film thicknesses and loads. Disappearance of stick-slip behavior would correspond to convergence of these two forces, i.e., to $F_{s(y)}-F_{s(\mathrm{sp})}\equiv\Delta F_s\rightarrow0$. We see at once from Figs. 14 and 15 that stick-slip behavior persists over the entire range of shear velocities studied. While there is some reduction (up to ca. 40%) in ΔF_s with initial increase in v_s, particularly for cyclohexane, its value levels out and remains finite up to the highest velocities studied.[57] We may estimate the values of the critical velocities by which the stick-slip behavior should have disappeared in our system, as given by Eq. (7). For our system, taking data for OMCTS from Fig. 12, for example, we have $\Delta F_s=5\times10^{-5}$ N, $K=K_1=300$ N/m, $F_{s(y)}=3\times10^{-4}$ N, $s=9$ Å $=9\times10^{-10}$ m, $M=20$ g$=0.02$ kg. This gives from Eq. (7), which is thought to fit better the behavior of simple liquids such as OMCTS and cyclohexane,[56] that $v_c=370$ nm/s, taking a value of 0.1 for the constant in Eq. (12). As seen in Fig. 12, stick-slip behavior clearly persists to very much higher shear velocities (to nearly 4000 nm/s), and indeed shows little sign of disappearing. For the OMCTS ($n=5$) data in Fig. 11, Eq. (7) would predict $v_c\approx70$ nm/s, but stick-slip behavior persists over the entire range of sliding velocities, to nearly 3000 nm/s. For cyclohexane too (Figs. 13 and 14) the stick-slip behavior persists to very much higher velocities than are pre-

dicted for its disappearance by Eq. (7). That is, our data do not support the prediction of Eq. (7) (indeed within the range of our parameters we observe no ''critical velocity'' at which the stick-slip behavior disappears). We note, however, that Eq. (7) was proposed on the basis of computer simulation studies at very different time scales,[55] and applying its predictions to the present experimental conditions involves extrapolation by several orders of magnitude and may not be justified. Finally, we remark that the simple picture for stick-slip friction introduced earlier is quite consistent with the existence of stick-slip motion up to very high sliding velocities.

Earlier experimental studies[20,21] of shear of highly compressed OMCTS layers ($n=1,2$) did suggest that the stick-slip of sheared OMCTS layers abruptly disappeared at a critical velocity whose magnitude was in accord with the prediction of Eq. (7). In these studies the compressive loads were substantially greater (in order to create larger contact areas and measureable shear forces), and the films consequently thinner, so that direct comparison with our own data, which does not agree with Eq. (7), may not be appropriate. It is also important to note that, due to the much higher resolution and sensitivity of the present shear force measurements, the magnitude of stick-slip effects (values of ΔF_s for example) which we could detect was extremely small. In particular, the ΔF_s values shown in Figs. 11–14 would not have been revealed in the earlier experiments,[20,21] even if stick-slip did remain beyond the point at which it was observed to have apparently disappeared at $v_s > v_c$.

V. SUMMARY

Using a surface force balance capable of simultaneous shear and normal force measurements we investigated the properties of thin films of a number of simple liquids. Our earlier paper (I) showed that an abrupt liquid-to-solid transition could be induced by confining the liquids to a certain critical film thickness equivalent to n_c monolayers of the liquids ($n_c=6$ for the cyclohexane and OMCTS used in these experiments). When in the solid phase ($n \leqslant n_c$), films of cyclohexane and OMCTS sheared via a characteristic stick-slip pattern, as observed in earlier studies. While the bulk of our results were for regimes of film thicknesses ($n=3-6$) and normal pressures not hitherto explored, we were able to make contact with earlier studies of thin films at one point of this regime ($n=3$). In this case the shear stresses of the solidlike confined films measured in the different studies agreed with each other within the scatter.

The shear stress required for sliding surfaces separated by these films varied with both thickness n of the film and with applied normal pressure. A simple model predicated on the requirement that sliding is initiated at the point where shear melting is first induced in the confined films was able to explain the frictional data satisfactorily. Most of the frictional dissipation mechanism in this model occurs at the point where the sheared film solidifies in the stick-slip cycle (very little is dissipated by viscous heating), and can account well for the external work required to slide the surfaces.

The variation of the shear stress required to slide the surfaces at a given normal pressure (or at zero pressure) was essentially independent of shear velocity over the range of our parameters. We also found that stick-slip behavior persisted over the entire range of shear velocities studied, up to values much higher than the velocities at which stick-slip was predicted and reported to disappear on the basis of earlier work. This may be due to the higher sensitivity of the present surface force balance in measuring shear forces.

ACKNOWLEDGMENTS

We thank R. Ball, H. Christensen, S. Granick, G. Grest, J. Israelachvili, M. Robbins, U. Landmann, Y. Rabin, S. Safran, and A. Weinstein for useful comments and correspondence, and U. Landman for providing us with a copy of Ref. 30 prior to publication. This work was supported by the Israel Science Foundation, the Ministry of Science and Arts (Israel-Tashtit programme) and the U.S.-Israel Binational Science Foundation.

[1] D. Tabor, *Friction* (Doubleday, New York, 1973).
[2] A. Vom Felde *et al.*, Phys. Rev. Lett. **53**, 922 (1984); C. Templier *et al.*, C.R. Acad. Sci. Paris **299**, 613 (1984); J. H. Evans and D. J. Marzey, J. Phys. F **15**, L1 (1985); M. W. Finnis, Acta Metall. **35**, 2543 (1987).
[3] H. K. Christenson, J. Chem. Phys. **78**, 6906 (1983).
[4] R. G. Horn and J. N. Israelachvili, J. Chem. Phys. **75**, 1400 (1981).
[5] J. S. Rowlinson and B. Widom, *Molecular Theory of Capillarity* (Clarendon Press, Oxford, 1982).
[6] F. P. Bowden and D. Tabor, *The Friction and Lubrication of Solids* (Clarendon Press, Oxford, 1964).
[7] *Fundamentals of Friction*, edited by I. L. Singer and H. M. Pollock (Kluwer Academic, The Netherlands, 1992).
[8] F. M. Etzler and W. Drost-Hansen, Adv. Chem. Ser. **188**, 486 (1980).
[9] H. M. Jaeger and S. R. Nagel, Science **255**, 1523 (1992).
[10] *Tribological Properties of Structural Ceramics*, edited by J. B. Wachtman, Jr. (Academic, San Diego, 1989); D. R. Clarke, Annu. Rev. Mater. Sci. **17**, 254 (1987) and references therein; J. E. Marion, C. H. Hsueh, and A. G. Evans, J. Am. Ceram. Soc. **70**, 708 (1987); D. Clarke, *ibid.* **70**, 15 (1987).
[11] L. T. Drzal, Adv. Polym. Sci. **75**, 1 (1985).
[12] S. Granick, Science **253**, 1374 (1991).
[13] J. F. Belak. Ed., *Nanotribology*, in Mater. Res. Soc. Bull. **18**, 15 (1993)
[14] A. I. Bailey and J. S. Courtney-Pratt, Proc. R. Soc. London, Ser. A **227**, 500 (1954).
[15] F. P. Bowden and D. Tabor, Proc. R. Soc. London, Ser. A **169**, 321 (1939).
[16] K. Kendall and D. Tabor, Proc. R. Soc. London, Ser. A **323**, 321 (1971).
[17] D. Tabor, Proc. Inst. Mech. Eng. **205**, 365 (1991).
[18] J. Israelachvili, P. M. McGuiggan, and A. M. Homola, Science **240**, 189 (1988).
[19] J. Van Alsten and S. Granick, Phys. Rev. Lett. **61**, 2570 (1988).
[20] M. L. Gee, P. M. McGuiggan, J. N. Israelachvili, and A. M. Homola, J. Chem. Phys. **93**, 1895 (1990).
[21] H. Yoshizawa and J. N. Israelachvili, J. Phys. Chem. **97**, 11300 (1993).
[22] G. Reiter, A. L. Demirel, and G. Granick, Science **263**, 1741 (1994).
[23] See review by N. Dan, Curr. Opin. Colloid Interface Sci. **1**, 48 (1996), and references therein.
[24] M. Schoen, C. Rhykerd, D. Diestler, and J. H. Cushman, Science **245**, 1223 (1989).
[25] P. A. Thompson and M. O. Robbins, Science **250**, 792 (1990).
[26] D. J. Diestler, M. Schoen, and J. H. Cushman, Science **262**, 545 (1993).
[27] I. Hersht and Y. Rabin, J. Non-Cryst. Solids **172-174**, 857 (1994).
[28] P. A. Thompson, M. O. Robbins, and G. S. Grest, Isr. J. Chem. **35**, 93 (1995).
[29] U. Landman, W. D. Luedtke, and M. W. Ribarsky, J. Vac. Sci. Technol. A **7**, 2829 (1989).
[30] J. Gao, W. D. Luedtke, and U. Landman, Phys. Rev. Lett. **79**, 705 (1997).
[31] M. Urbakh, L. Daikhin, and J. Klafter, Europhys. Lett. **32**, 125 (1995).
[32] J. H. Cushman, Nature **347**, 227 (1990).
[33] J. Klein and E. Kumacheva, Science **269**, 816 (1995).

[34] J. Klein and E. Kumacheva, J. Chem. Phys. **108**, 6996 (1997), preceding paper.
[35] S. Toxvaerd, J. Chem. Phys. **74**, 1998 (1981).
[36] As explained in paper I (Ref. 34), the contact area $\mathscr{A}$ arises from deformation of the contacting curved surfaces due to the applied load and the attraction between them. It is evaluated via the JKR model of contact mechanics (Ref. 37). $\mathscr{A}=\pi a^2$, where a is the radius of the circular contact area given by

$$a^3=\frac{R}{K}[F_n+2F_p+2(F_nF_p+F_p^2)^{1/2}].$$

Here $R=(R_1R_2)/(R_1+R_2)$ for contact between crossed cylinders of radii R_1, R_2; K is related to the Youngs modulus of the cylinders (assumed to be of the same material); and F_p is the pull-off force required to separate the two surfaces against the adhesion force between them (Fig. 1).
[37] K. L. Johnson, K. Kendall, and A. D. Roberts, Proc. R. Soc. London, Ser. A **324**, 301 (1971).
[38] From Fig. 9 in Gee *et al.* (Ref. 20) the critical shear stress for OMCTS at $n=3$ and a normal load $L=(2.5\pm1)$ mN is 1.10^6 N/m^2. The corresponding pressure is $P=L/\mathscr{A}$, where the contact area $\mathscr{A}$ for this load is taken from Fig. 3 in Homola *et al.* (Ref. 53).
[39] Hu *et al.* (Ref. 40) have also reported values for the shear stress between mica surfaces sliding at different velocities across an OMCTS film confined to thickness $n=3$, at shear rates and normal pressures comparable to those in the present study. Their results, however [and also a more recent study from the same group (Ref. 41)], indicated viscous rather than solidlike response (no yield stress at zero frequency was observed), and so contrast with our data as well as with the data of Gee *et al.* (Ref. 20) and Yoshizawa and Israelachvili (Ref. 21). Possible reasons for the discrepancy have been considered in paper I (Ref. 34, preceding paper).
[40] H.-W. Hu, G. A. Carson, and S. Granick, Phys. Rev. Lett. **66**, 2758 (1991).
[41] A. L. Demirel and S. Granick, Phys. Rev. Lett. **77**, 2261 (1996).
[42] M. G. Rozman, M. Urbakh, and J. Klafter, Phys. Rev. Lett. **77**, 683 (1996).
[43] J. Gao, W. D. Luedtke, and U. Landman, J. Chem. Phys. **106**, 5751 (1997).
[44] O. Reynolds, Philos. Mag. **8**, 22 (1885).
[45] B. J. Briscoe and D. C. B. Evans, Proc. R. Soc. London, Ser. A **380**, 389 (1982).
[46] D. Tabor, in *Microscopic Aspects of Adhesion and Lubrication, Tribology Series 7*, edited by J. M. Georges (Elsevier, New York, 1982), pp. 651–682.
[47] B. J. Briscoe and D. Tabor, J. Adhesion **9**, 145 (1978).
[48] H. Yoshizawa and J. N. Israelachvili, Thin Solid Films **246**, 71 (1994).
[49] Similar ideas concerning the shear melting of bulk crystalline solids were discussed long ago [J. Frenkel, *Kinetic Theory of Liquids* (Clarendon Press, Oxford, 1946)].
[50] A treatment somewhat in this spirit for shear of powder particles was presented by M. J. Adams (Ref. 7, p. 183) though in this model the friction between the powder particles themselves played a central role.
[51] J. Klein, J. Non-Cryst. Solids (to be published).
[52] S. Granick, A. L. Demirel, L. L. Cai, and J. Peanasky, Isr. J. Chem. **35**, 75 (1995).
[53] A. M. Homola, J. N. Israelachvili, M. L. Gee, and P. M. McGuiggan, J. Tribology **111**, 675 (1989).
[54] R. W. K. Honeycombe, *The Plastic Deformation of Metals* (Arnold, London, 1984).
[55] M. O. Robbins and P. A. Thompson, Science **253**, 916 (1991).
[56] An alternative expression for v_c was subsequently suggested (Ref. 21) but is not considered here as Eq. (7) is thought to be more suited for liquids consisting of simple spherical molecules (Ref. 21).
[57] Stick-slip is strictly observed only at frequency $\nu<\nu_{\text{resonance}}$ of the shear spring/mounting assembly, $=17$ Hz. Thus Fig. 10(A) shows stick-slip (at $\nu<\nu_{\text{resonance}}$) for v_s up to 2000 nm/s, but for Fig. 10(B), $v_s=3500$ nm/s, the frequency of the apparent stick-slip signal has saturated at $\nu_{\text{resonance}}$ of the shear-spring assembly (Ref. 34).
[58] This contrasts with the reported (2/3) power-law variation of effective viscosity with shear rate (determined as above from the Newtonian definition), $\eta_{\text{eff}}\propto\dot{\gamma}^{-2/3}$, which was reported earlier (Ref. 40) for shear of some confined liquids, including thin films ($n=3$) of OMCTS. The reasons for the discrepancy have been discussed [see Ref. 39 and our preceding paper I (Ref. 34)].